

Mass measurements on neutron-deficient Sr and neutron-rich Sn isotopes with the ISOLTRAP mass spectrometer

G. Sikler^{a,*}, G. Audi^b, D. Beck^c, K. Blaum^d, G. Bollen^e,
F. Herfurth^c, A. Kellerbauer^f, H.-J. Kluge^c, D. Lunney^b,
M. Oinonen^g, C. Scheidenberger^c, S. Schwarz^e, J. Szerypo^h,
C. Weber^d

^a*MPI für Kernphysik, Saupfercheckweg 1, 69117 Heidelberg, Germany*

^b*CSNSM-IN2P3-CNRS, Bâtiment 108, 91405 Orsay-Campus, France*

^c*GSI, Planckstr.1, 64291 Darmstadt, Germany*

^d*Johannes Gutenberg-Universität Mainz, Staudingerweg 7, 55128 Mainz, Germany*

^e*NSCL, Michigan State University, East Lansing, MI 48824-1321, USA*

^f*CERN, 1211 Geneva 23, Switzerland*

^g*Helsinki Institute of Physics, P.O. Box 64, 00014 University of Helsinki, Finland*

^h*LMU München, Am Coulombwall 1, 85748 Garching, Germany*

Abstract

The atomic masses of $^{76,77,80,81}\text{Sr}$ and $^{129,130,131,132}\text{Sn}$ were measured by means of the Penning trap mass spectrometer ISOLTRAP at ISOLDE/CERN. ^{76}Sr is now the heaviest $N = Z$ nucleus for which the mass is measured to a precision better than 35 keV. For the tin isotopes in the close vicinity of the doubly magic nucleus ^{132}Sn , mass uncertainties below 20 keV were achieved. An atomic mass evaluation was carried out taking other experimental mass values into account by performing a least-squares adjustment. Some discrepancies between older experimental values and the ones reported here emerged and were resolved. The results of the new adjustment and their impact will be presented.

Key words: atomic masses, strontium, tin, high-precision mass spectrometry, ISOLTRAP

PACS: 07.75.+h, 21.10.Dr, 32.10.Bi

* Corresponding author.

Email address: g.sikler@mpi-hd.mpg.de (G. Sikler).

1 Introduction

Doubly-magic nuclei form a basis for the nuclear shell model and are also an important concept in testing the models describing the bulk properties of nuclei. The description of shell closure and its disappearance for exotic nuclei, the so-called shell quenching [1, 2], is one main issue in each nuclear theory. As the number of valence nucleons increases, the shapes of the nuclei tend to turn from a spherical configuration (doubly-magic) to extreme deformations. Particularly, the $N \approx Z$ nuclei have been of special interest since the early days of investigating the structure of atomic nuclei [3, 4]. Following the concept of valence nucleons and mirror nuclei this region is still a unique test bench for investigating the forces between individual nucleons as well as their interactions with the residual nuclear core [5, 6]. Furthermore, strong deformations among the upper fp-shell $N \approx Z$ nuclei have particularly triggered development of new methods for deducing the nature of ground-state deformations [7, 8]. It is of central relevance whether the theoretical predictions remain valid when extending them into formerly unknown regions far from the valley of β -stability. The very heavy $N = Z$ nuclei are of additional importance due to their key role in the astrophysical rp- (rapid proton capture) process [9] and their close vicinity to the proton drip line. A key quantity allowing the comparison of theoretical models and measured values is the ground state binding energy, and hence the atomic mass. In the last decade, great progress both in the production and preparation of exotic nuclides [10] as well as in the improvement of mass-measurement techniques [11] was achieved. The mass measurements reported here were performed using the Penning trap mass spectrometer ISOLTRAP [12] at the on-line isotope separator ISOLDE [13] located at CERN in Geneva, Switzerland. Here the mass determination is linked to the measurement of the cyclotron frequency $\nu_c = qB/(2\pi m)$ of an ion being confined in a Penning trap. This frequency governs the motion of an ion with charge q and mass m circulating in a magnetic field of strength B . Thus, for a known charge state the mass can be determined by measuring the cyclotron frequency ν_c and the magnetic field B . In the following the experimental setup of the ISOLTRAP mass spectrometer is explained and the mass measurements for the nuclides $^{76,77,80,81}\text{Sr}$ and $^{129,130,131,132}\text{Sn}$ are described. The results are compared with literature values and their influence on the surrounding mass surface is discussed.

2 Setup and Experimental Procedure

At ISOLDE radionuclides are produced in one of the two target stations by an intense beam of protons impinging with a kinetic energy of up to 1.4 GeV. The radionuclides are created in induced fission and spallation reactions and diffuse into an ion source. From here the positively charged ions get electrostat-

ically accelerated to 60 keV and mass-selected by one (GPS, general-purpose separator) or a set of two (HRS, high-resolution separator) magnets. Afterwards the ions are transported to the various experiments, one of which is the ISOLTRAP mass spectrometer.

ISOLTRAP (Fig. 1) uses three different ion traps to perform the mass measurement procedure. The first one is a gas-filled, linear radiofrequency quadrupole (RFQ) structure, which is used for stopping, cooling, and accumulating the ions [14]. The second trap is a gas-filled, cylindrical Penning trap where isobaric contaminants can be removed [15]. Finally the cyclotron frequency of the ions is measured in the hyperbolically shaped precision Penning trap.

As the ions enter the RFQ buncher they get decelerated by a retarding electric field from 60 keV down to about 100 eV. To the four rods of the linear quadrupole structure a radiofrequency field is applied, which keeps the ions radially confined. Each rod is longitudinally cut into 26 electrically insulated segments. By applying DC voltages (in addition to the RF component) to the different segments a potential well is created along the longitudinal axis. The structure is filled with helium buffer gas at a pressure of about 10^{-3} to

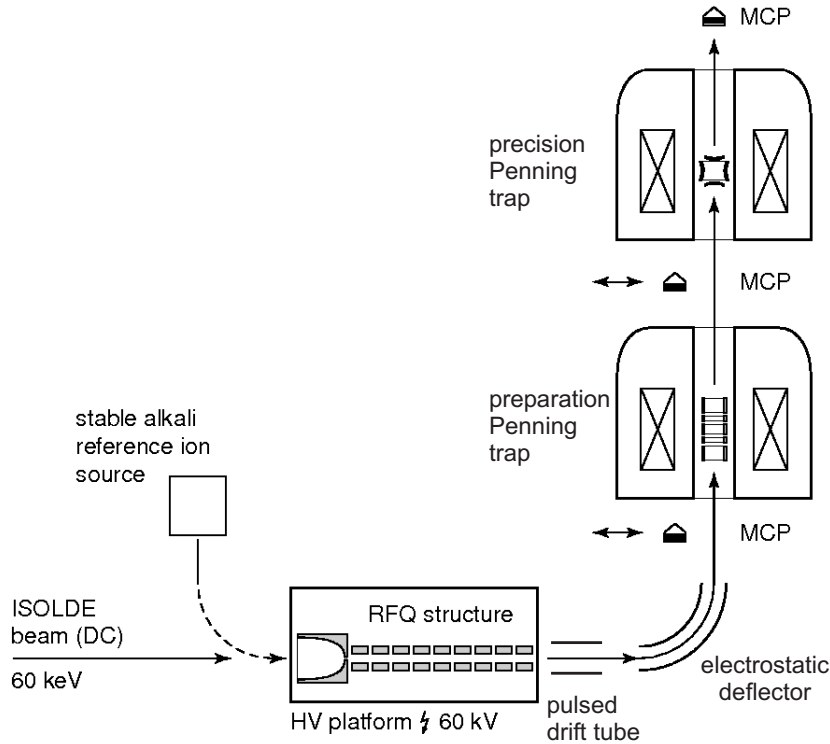


Fig. 1. Sketch of the precision mass spectrometer ISOLTRAP. The experimental setup consists of three traps: A linear Paul trap, a preparation Penning trap for beam cooling, and isobaric separation and a precision Penning trap for the cyclotron frequency measurement.

10^{-2} mbar. Due to collisions with the buffer gas the ions lose kinetic energy. They are cooled into the minimum of the effective potential created by the applied DC and RF voltages. By switching down the DC potentials at the exit end of the buncher the ions are extracted out of the device. The bunch gets transported to the first Penning trap after the kinetic energy of the ensemble is matched to the trap potential in a pulsed drift tube.

The ISOLTRAP preparation trap is a cylindrical Penning trap [15] which is filled with helium as a buffer gas at a pressure of about 10^{-5} to 10^{-4} mbar. The ring electrode is radially split to enable azimuthal RF fields to be radiated into the trap volume. By using buffer gas and radial fields alternating at the cyclotron frequency of a particular ion species, only these ions are kept confined in the trap center [16]. Adjusting the proper frequency for the azimuthal RF field and extracting the ions through a small diaphragm out of the trap provides a selection of a particular ion species. With the ISOLTRAP preparation trap a mass resolving power of up to $R = m/\Delta m_{\text{FWHM}} \approx 10^5$ has been achieved [15]. The removal of isobaric contaminant ions is a vital requirement for measuring the cyclotron frequency to a high precision (see section 3). In some cases the contaminations exceed the number of ions of interest by such a big amount that the mass-selective buffer-gas cooling is not sufficient to remove all unwanted species completely. In such a case another cleaning procedure is applied to the ensemble after its transfer into the precision trap. This one is a hyperbolic Penning trap with a four-fold segmented ring electrode. By applying across two opposite lying segments a dipolar field alternating with the reduced cyclotron frequency of the unwanted ions, they are driven to large radial orbits so as to no longer affect the motion of the ions of interest.

The ISOLTRAP precision trap is used to measure the cyclotron frequency of the radionuclides using a resonant time-of-flight (TOF) technique [17]. The segmentation of the ring electrode allows one to create an azimuthal quadrupolar RF field. Such a field is used to excite the motion of the ions in their radial degree of freedom. The excitation is resonant when the RF equals the cyclotron frequency of the trapped ions. When they are extracted out of the trap by lowering the potential applied to the upper end electrode the ions leave the magnetic field as well. Due to the coupling of the cyclotron motion to the magnetic field gradient, the initially radial kinetic energy is converted into axial kinetic energy. The larger the radial energy is prior to the extraction, the stronger will be the axial acceleration. A microchannel plate (MCP) detector placed 1.2 m above the trap on the axis outside the magnetic field is used to determine the time of flight of the ions after their extraction out of the trap. The determination of the mean time of flight is a measure for the initial radial kinetic energy. If the ions are excited resonantly at their cyclotron frequency the time of flight is minimal.

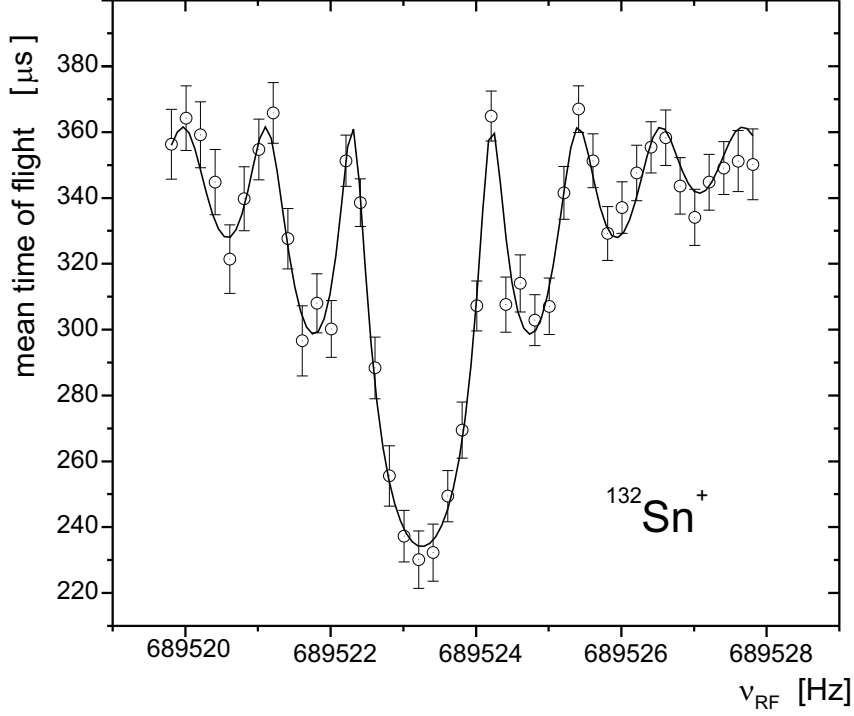


Fig. 2. Time-of-flight spectrum for $^{132}\text{Sn}^+$. The time of flight of the ions is displayed as a function of the frequency of the radial excitation. The solid line results from a fit of the theoretical line shape to the data points. The minimum in the time of flight appears at the cyclotron frequency ν_c .

Figure 2 displays a typical time-of-flight resonance spectrum as it was obtained for $^{132}\text{Sn}^+$ during the reported set of measurements. The width of the resonance depends mainly on the duration of the RF excitation T_{RF} and is $\Delta\nu_{\text{FWHM}} \approx 1/T_{\text{RF}}$. By fitting the theoretically expected line shape [18] to the data points, the cyclotron frequency and its standard deviation are determined. To obtain an accurate value for the mass of the ions of interest, the strength of the magnetic field needs to be determined precisely. Before and after the ν_c measurement of the ion of interest the B -field calibration is done by measuring the cyclotron frequency of stable ions of well-known mass, applying the same technique as described above. For this purpose and for testing the apparatus an off-line ion source for alkaline elements is attached to the experiment. If m_{ref} is the mass of the reference atom and m_e the electron mass, the atomic mass of a radionuclide m_{rad} can be determined from the cyclotron frequencies ν_{ref} and ν_{rad} of the singly-charged corresponding ions:

$$m_{\text{rad}} = \frac{\nu_{\text{ref}}}{\nu_{\text{rad}}} \cdot (m_{\text{ref}} - m_e) + m_e . \quad (1)$$

The atomic masses of about 300 radionuclides were measured at ISOLTRAP until now with a typical relative uncertainty of $1 \cdot 10^{-8} < \frac{\Delta m}{m} < 5 \cdot 10^{-7}$.

3 Mass Measurements on neutron-deficient Sr- and neutron-rich Sn-isotopes

A 1.4-GeV proton beam impinging on a niobium target was used to create the investigated neutron-deficient Sr isotopes. The ionization took place on a heated tungsten surface, from which also stable Rb isotopes were released and ionized. In the case of the most exotic of the investigated Sr isotopes ($^{76,77}\text{Sr}$), the amount of the isobars $^{76,77}\text{Rb}^+$ exceeded the quantity of Sr by a factor of $5 \cdot 10^3$ to $5 \cdot 10^4$. Due to space charge limitations, the ISOLTRAP preparation trap is not suitable for removing contaminants of this large rate in an effective manner. Nevertheless, to make those isotopes accessible to a mass measurement, CF_4 gas was introduced into the ion source to form SrF^+ molecular ions. In their mass range ($A = 95, 96$) no high-rate contaminants (in particular no RbF^+) were observed. Fluorine was chosen for the molecule formation because of its high chemical reactivity and the fact that there is only one stable F isotope. Furthermore, the mass of ^{19}F is known with a relative uncertainty of $\frac{\Delta m}{m} = 3.9 \cdot 10^{-9}$ [19]. Hence, this small uncertainty does not contribute to the mass determination of the respective Sr isotopes. The molecular binding energy, in the order of a few eV, is also negligible for the desired accuracy.

The production of the neutron-rich Sn isotopes occurred in fission of uranium induced by bombardment with 1.4 GeV protons. The usage of the ISOLDE resonance ionization laser ion source (RILIS) allowed for an element-specific selection in addition to the mass separation. To achieve a fast and effective diffusion of the radionuclides, the target container was heated to a temperature of about 2000°C. By this Cs and Ba isotopes were also released and ionized.

A list of the investigated nuclides is given in table 1 with their nuclear half-lives and their production rates at ISOLDE. The access to even more exotic, neutron-deficient Sr isotopes was mainly limited by the production rate, which was less than 100 ions per proton pulse for ^{75}Sr . For the tin measurements, contamination by surface-ionizable isobars inhibited the mass determination of isotopes further away from the valley of stability. The production rate of *e.g.* $^{133}\text{Cs}^+$ exceeded the one for $^{133}\text{Sn}^+$ by at least five orders of magnitude.

After the production, ionization, separation, and transport of the radionuclides, the ions were accumulated in the ISOLTRAP RFQ buncher. The cooling process in the buncher took about 10 to 20 ms and cooling and cleaning in the preparation Penning trap lasted for 300 ms. In spite of the purification in the preparation trap during all Sn measurements, isobaric Cs and Ba contaminants were found to be present in the precision Penning trap. They were driven to large radii as described in section 2 by applying the dipolar cleaning RF-signal for 300 ms. The excitation of the cyclotron motion was

Table 1

List of the investigated strontium and tin isotopes. The values for the excitation energies of the isomeric states in the second column and for the half-lives in the third column are taken from [20]. For the isotopes $^{129,130,131}\text{Sn}$, the values for the production rates include both, nuclei in the ground state as well as in the long-lived isomeric state.

ion	E_{excit} [keV]	$T_{1/2}$	ions per proton pulse
$^{76}\text{Sr}^{19}\text{F}^+$		8.9 s	$4 \cdot 10^3$
$^{77}\text{Sr}^{19}\text{F}^+$		9.0 s	$2 \cdot 10^5$
$^{80}\text{Sr}^+$		106.3 m	$1 \cdot 10^9$
$^{81}\text{Sr}^+$		22.3 m	$3 \cdot 10^9$
$^{86}\text{Sr}^{19}\text{F}^+$		stable	$2 \cdot 10^{10}$
$^{88}\text{Sr}^+$		stable	$3 \cdot 10^9$
$^{124}\text{Sn}^+$		stable	$> 1 \cdot 10^9$
$^{129g}\text{Sn}^+$		2.23 m	} $3.2 \cdot 10^8$
$^{129m}\text{Sn}^+$	35.2 (3)	6.9 m	
$^{130g}\text{Sn}^+$		3.72 m	} $3.8 \cdot 10^8$
$^{130m}\text{Sn}^+$	1 946.88 (10)	1.7 m	
$^{131g}\text{Sn}^+$		56 s	} $2.9 \cdot 10^8$
$^{131m}\text{Sn}^+$	242.8 (8)	58.4 s	
$^{132}\text{Sn}^+$		39.7s	$1.6 \cdot 10^8$

applied for $T_{\text{RF}} = 900$ ms resulting in a resonance width of $\Delta\nu_{\text{FWHM}} \approx 1.4$ Hz. This translates into a resolving power of $R \approx 800\,000$ for the investigated Sr isotopes and $R \approx 540\,000$ for the Sn measurements. The whole measurement cycle was repeated for 41 different frequencies around the expected cyclotron frequency. Each frequency step was 0.2 Hz wide covering a scan range of 8 Hz in total. To decrease the statistical uncertainty of the mean time of flight for each frequency step, the scanning procedure was repeated a few ten times. The total number of detected ions per TOF resonance was on average about 2500. For most of the radionuclides the center frequency could be determined with a relative statistical uncertainty of $2 \cdot 10^{-8} < \frac{\sigma_{\text{stat}}}{\nu_c} < 8 \cdot 10^{-8}$. For ^{76}Sr it was only $\frac{\sigma_{\text{stat}}}{\nu_c} = 3.6 \cdot 10^{-7}$ due to the low production rate.

Despite the fact that mass-selective buffer-gas cooling was applied and the residual stable Cs and Ba isobars were excited to large cyclotron radii in the precision trap, their influence on the cyclotron-frequency measurement of the investigated Sn isotopes could not be fully suppressed. The presence of contaminant ions of different mass during the cyclotron excitation introduces

a perturbation of the ions' motion, resulting in a systematic, negative shift of the measured cyclotron frequency. The shift depends upon the amount of impurity ions. Assuming a constant number ratio of wanted and unwanted ions throughout the measurement, the frequency shift gets larger with increasing number of ions in the trap. During the evaluation, event cycles were grouped into classes being characterized by the count rate Z . For each Z -class individual TOF-resonance spectra were created and the respective cyclotron frequencies determined. Examining ν_c as function of the count rate uncovered a small but systematic change for all the Sn data. Correcting these frequency shifts was accompanied by an increase in the uncertainty by a factor of 2 to 5, depending on the isotope. No count-rate-dependent frequency shifts were observed for the Sr isotopes and the reference nuclides, as expected.

$^{85}\text{Rb}^+$ ions were chosen for magnetic field calibration during the Sr measurements whereas $^{133}\text{Cs}^+$ was used as reference for the Sn run. The relative mass uncertainties for these stable isotopes are $1.4 \cdot 10^{-10}$ for ^{85}Rb and $1.8 \cdot 10^{-10}$ in the case of ^{133}Cs , respectively [21]. The choice of the reference ions is also determined by the requirement to have the reference mass as close as possible to the mass of interest in order to minimize mass dependent uncertainties. Field imperfections, *i.e.* inhomogeneity of the magnetic field, inharmonicity of the electric field and a misalignment of the two with respect to each other are sources for systematic errors in the measurement of the cyclotron frequency. The latter imperfection in particular may cause a relative deviation $\frac{\delta r}{r} \propto \Delta m$ of the frequency ratio $r = \nu_{\text{rad}}/\nu_{\text{ref}}$ which is (to first-order approximation) linear with the difference $\Delta m = |m_{\text{rad}} - m_{\text{ref}}|$ between the mass of the ion under investigation and the reference ion. The shift of the frequency ratio due to this mass difference was found to be $(\Delta r/r)_{\Delta m} = 1.6(4) \cdot 10^{-10}/u \cdot \Delta m$ [22] for the ISOLTRAP precision trap. With the choice of ^{85}Rb as reference for

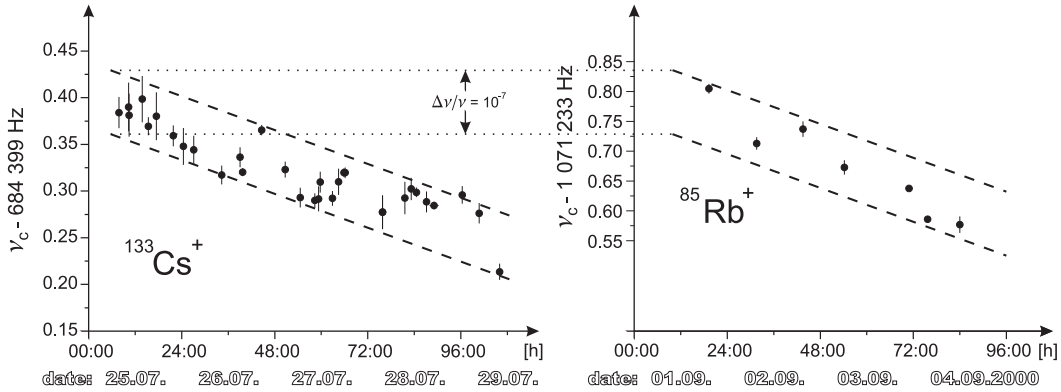


Fig. 3. Temporal magnetic field drift during the Sn and Sr experiments. All reference cyclotron-frequency measurements on $^{133}\text{Cs}^+$ (left) and $^{85}\text{Rb}^+$ (right) are displayed. The B -field decreases constantly by about $\frac{\Delta B}{B} \approx 5.3 \cdot 10^{-8}$ per 24 hours. The short term fluctuations stay within an area of $\frac{\Delta B}{B} \leq 10^{-7}$, indicated by the dashed lines. The frequency scale of the diagram to the right is compressed by the mass ratio factor $\frac{133}{85} = 1.56$.

the Sr measurement, the mass difference Δm is at most 11 u. The contribution to the relative systematic uncertainty of the frequency ratio amounts to $(\Delta r/r)_{\Delta m} < 2.2 \cdot 10^{-9}$. For the tin isotopes the difference to the reference ion ^{133}Cs is at most 4 u, hence the contribution to the uncertainty is only $(\Delta r/r)_{\Delta m} < 8 \cdot 10^{-10}$.

The most critical known systematic error stems from the temporal magnetic field drift during the measurement. If the cyclotron frequency of the reference ion is measured for a different B -field strength than that of the radionuclide, the frequency ratio is incorrect. Figure 3 displays all cyclotron-frequency measurements for the reference nuclides as obtained during the Sn (left) and the Sr run (right) as a function of time. Besides the global decrease, short term fluctuations are observed. The deviations stay within a narrow band, which has a relative width of $\frac{\Delta\nu}{\nu} \leq 10^{-7}$. The difference between each pair of neighboring measurements is on average only $\leq 3 \cdot 10^{-8}$.

In table 2 all systematic errors are listed and an upper limit is estimated for each of them. A relative uncertainty of $\frac{\Delta\nu}{\nu} = 10^{-7}$ was added quadratically to the statistical uncertainty as it was obtained from the fit to the experimental TOF spectra and corrected to cover contaminations in the tin measurements. The overall uncertainty

$$\left(\frac{\Delta r}{r}\right)_{tot} = \sqrt{\left(\frac{\sigma_{\text{stat}}(r)}{r}\right)^2 + (10^{-7})^2} \quad (2)$$

Table 2

List of all considered systematic errors. Adding a relative uncertainty of 10^{-7} to the statistical one covers in a conservative way all possible systematic errors.

systematic error	contribution to the relative uncertainty $\frac{\Delta m}{m}$
contaminations (only for Sn)	corrected; included in σ_{stat}
$B(t) \neq \text{const}$	in average $\approx 3 \cdot 10^{-8}$
$(m_{\text{ref}} - m_{\text{rad}}) \neq 0$	$< 8 \cdot 10^{-10}$ (Sn), $< 2.2 \cdot 10^{-9}$ (Sr)
$(\Delta m/m)$ of the reference ion	$1.8 \cdot 10^{-10}$ (Cs), $1.4 \cdot 10^{-10}$ (Rb)
binding energy of missing electron	$< 10^{-10}$
$(\Delta m/m)$ of an electron	$< 10^{-14}$
total	$< \sqrt{\left(\frac{\sigma_{\text{stat}}}{m}\right)^2 + (10^{-7})^2}$

is believed to cover all possible errors. Besides the radionuclides for each species (Sn^+ , Sr^+ , and SrF^+), the mass of a stable representative was measured for cross check. The good agreement with the more accurate literature values (see section 4) underlines the absence of additional, undetected systematic errors during the measurements.

4 Results and Discussion

In table 3 the frequency ratios $r = \nu_{\text{ref}}/\nu_{\text{rad}}$, the obtained atomic masses m_{atom} , and the mass-excess values (ME) are listed for the investigated nuclides. The ME is defined to be:

$$\text{ME}[\text{u}] = m_{\text{atom}}[\text{u}] - A, \quad (3)$$

where m_{atom} is the atomic mass of the nuclide and A its mass number.

Each of the nuclides $^{129,130,131}\text{Sn}$ has an excited isomeric state (see table 1) requiring additional considerations concerning the deduced ME-values. The isomeric state of ^{129}Sn has an excitation energy of 35.2(0.3) keV. This small difference in binding energy cannot be resolved in the ISOLTRAP precision Penning trap using reasonable excitation times of a few seconds. Therefore the measured atomic mass has to be considered as a mixture of the ground-state mass and the one for the excited state. Under the assumption that both isomers are produced with the same rate, the measured ME is the average of the value for the ground state and the one for the excited state. Hence the value for the measured ground state ME is corrected by half the excitation energy, 17.6 keV. To account for the uncertainty in the relative production ratio of the two states, an additional error of 10 keV is added quadratically to the uncertainty of the ME, yielding a corrected value of $\text{ME}(^{129g}\text{Sn}) = -80\,594(29)$. In the case of ^{130}Sn the isomeric states could be resolved individually. The difference between the atomic masses of ground and isomeric state (see table 3) is $m(^{130m}\text{Sn}) - m(^{130g}\text{Sn}) = 1\,944(19)$ keV. This is in good agreement with the value for the excitation energy $E_\gamma = 1\,946.88(10)$ keV [27] obtained in a γ -spectroscopy measurement. Due to this good agreement, the mass value for the excited state could be used to improve the value for the ground state to be $\text{ME}(^{130g}\text{Sn}) = -80\,136(10)$ keV. For ^{131}Sn the isomeric state has an excitation energy of $E_\gamma = 241.8(8)$ keV [28]. During the measurements presented here the two isomeric states could not be resolved. Even with an excitation time of $T_{\text{RF}} = 2$ s, which is equivalent to a mass resolving power of $\Delta m \approx 105$ keV, no signature for two individual states could be seen (Fig. 4). Either one of the isomeric states was not produced or the excitation energy is in fact smaller than ≈ 100 keV. The half-lives of the two states are similar (see table 1)

Table 3

Frequency ratios r and atomic masses of the investigated Sr- and Sn-isotopes. During the Sr run ^{85}Rb ($m_{\text{atom}} = 85\,911\,789.732(14) \mu\text{u}$ [21]) was used as a reference nuclide and the Sn measurements were calibrated with ^{133}Cs ($m_{\text{atom}} = 132\,905\,451.931(27) \mu\text{u}$ [21]). The column labeled N_{tot} gives the total amount of ions which contributed to the particular measurement. The frequency ratios together with the corresponding total uncertainty are listed in column r . For the atomic masses of those Sr isotopes for which the cyclotron frequency of the molecular ions SrF^+ was measured, the mass of ^{19}F ($m_{\text{atom}} = 18\,998\,403.205(75) \mu\text{u}$ [23]) is already subtracted. In the last column the values for the mass excess ME are displayed. For the conversion from the atomic mass unit u into keV the relation $1 \mu\text{u} \hat{=} 931.494012 \text{ eV}$ [24] was used.

reference	ion	N_{tot}	$r = \nu_{\text{ref}}/\nu_{\text{rad}}$	$m_{\text{atom}}[\mu\text{u}]$	ME [keV]
^{85}Rb	$^{76}\text{Sr}^{19}\text{F}^+$	1636	1.11810422(43)	75 941 765(37)	-54 249(34)
	$^{77}\text{Sr}^{19}\text{F}^+$	2954	1.12983627(10)	76 937 945 (8)	-57 804 (8)
	$^{80}\text{Sr}^+$	600	0.94126475(17)	79 924 506(15)	-70 322(14)
	$^{81}\text{Sr}^+$	960	0.95302645(14)	80 923 207(12)	-71 532(11)
	$^{86}\text{Sr}^{19}\text{F}^+$	8301	1.23549153(15)	85 909 264(12)	-84 520(12)
	$^{88}\text{Sr}^+$	1957	1.03525828(13)	87 905 614(11)	-87 920(10)
^{133}Cs	$^{124}\text{Sn}^+$	6970	0.93228114(16)	123 905 283(21)	-88 228(20)
	$^{129g,m}\text{Sn}^+$	5259	0.96996383(22)	128 913 498(29)	-80 576(27)
	$^{130g}\text{Sn}^+$	13223	0.97749158(13)	129 913 972(17)	-80 134(16)
	$^{130m}\text{Sn}^+$	6123	0.97750729 (9)	129 916 059(12)	-78 190(11)
	$^{131g,m}\text{Sn}^+$	8159	0.98503912(12)	130 917 077(16)	-77 242(15)
	$^{132}\text{Sn}^+$	11847	0.99256895(14)	131 917 829(18)	-76 542(17)

and very long compared to the measurement cycle. Neither the production mechanism nor the ionizing process is known to favor one state compared to the other. To account for the lack of knowledge about which state was observed, a correction, like in the case of ^{129}Sn , was made. The corrected value for the ground state mass excess of ^{131g}Sn is $\text{ME}(^{131g}\text{Sn}) = -77\,363(72) \text{ keV}$.

The new ISOLTRAP values were included into the most recent atomic-mass evaluation (AME2003) [25], resulting in new ME values for some of the investigated nuclides. In table 4 the ME values given by the AME after the readjustment ($\text{ME}_{\text{AMEnew}}$) are compared with the ones as stated before ($\text{ME}_{\text{AMEold}}$). The ISOLTRAP data (ME_{IST}) for some Sn isotopes differ from those in table 3, because they incorporate the corrections discussed above. In the last column of table 4 the contribution of the presented data to the new adjustment is indicated.

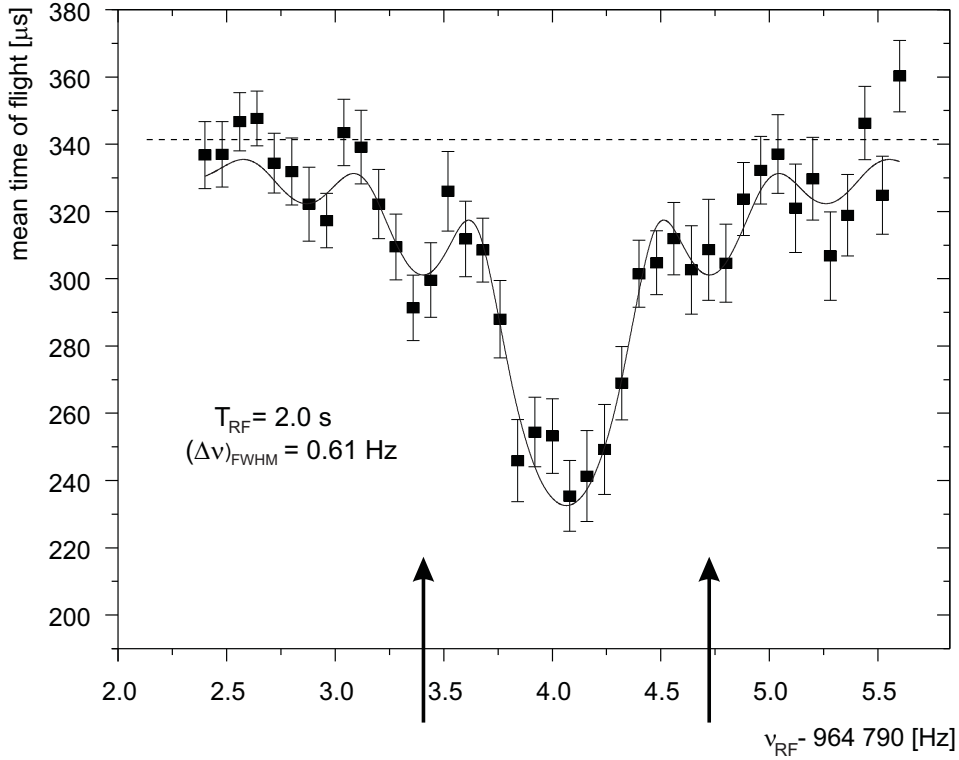


Fig. 4. TOF-resonance-spectrum for ^{131}Sn . The spectrum was obtained using an excitation time of $T_{\text{RF}} = 2.0$ s. The arrows 1.3 Hz left and right of the TOF minimum indicate the position of an expected resonance for a second state which is 240 keV lighter or heavier than the observed one. There is clearly no evidence for such a state.

The uncertainty of our data for the stable nuclides $^{86,88}\text{Sr}$ and ^{124}Sn is too large to have any impact on the respective recommended value. Nevertheless they are useful to check for possible, undetected systematic errors (see section 3). The masses of the Sr isotopes $^{80,81}\text{Sr}$ were previously measured at ISOLTRAP [26]. The new data are in very good agreement with the previous values and help to reduce the uncertainty of the recommended values slightly. In the case of ^{77}Sr , the trap value allows a decrease in the uncertainty by almost a factor of 20. The other contributing experimental data were all determined in nuclear decay energy measurements. The ME of ^{76}Sr stated here is the only experimental value which is included into the AME until now.

The previous AME values for the neutron-rich tin isotopes were all based on measurements of Q_{β} -values. The data reported here do not depend on the knowledge of decay schemes, excitation energies and masses of daughter nuclides. They agree well (except for ^{130}Sn) with the β -spectroscopy data. Including them into the mass evaluation led to a decrease of the uncertainties in most of the cases.

The previous AME value for ^{129}Sn was determined by Q_β -measurements only, which linked the ground-state binding energy of this nuclide via the β -decay chain $^{129}\text{Sn} \rightarrow ^{129}\text{Sb} \rightarrow ^{129}\text{Te}$ to the mass of ^{129}Te which has an uncertainty of $\Delta m = 3$ keV. Despite the fact that the isomeric state could not be resolved in the measurement reported here, it is more accurate and hence the leading contribution in the new adjustment, being in good agreement with the previous one.

A significant disagreement of 3.3 standard deviations from the previous AME value was found for ^{130}Sn . The old value was linked to the mass of the stable isobar ^{130}Te ($\Delta m(^{130}\text{Te}) = 2$ keV) by several Q_β -measurements [29–33]. The weighted mean values $Q(\text{Sn} \rightarrow \text{Sb}) = 2\,148(15)$ keV and $Q(\text{Sb} \rightarrow \text{Te}) = 4\,972(22)$ keV add up to a sum of $7\,120(26)$ keV, whereas the difference of the directly measured masses of ^{130}Sn from this work and ^{130}Te from the AME is as much as $m(\text{Sn}) - m(\text{Te}) = 7\,217(16)$ keV. A detailed survey of the Q_β contributions revealed that the assumed decay schemes used for the various β energy-spectra assignments were not the same in all the references. After

Table 4

Comparison of the new ISOLTRAP data with those given by the AME before. For each nuclide the value for the mass excess as determined in this work (ME_{IST}) is given. In addition the values as given by the atomic-mass evaluation including ($\text{ME}_{\text{AMEnew}}$) and not including ($\text{ME}_{\text{AMEold}}$) the ISOLTRAP data are displayed. In the last column the influence of the ISOLTRAP data on the new recommended ME-values are listed.

nuclide	ME_{IST} [keV]	$\text{ME}_{\text{AMEold}}$ [keV]	$\text{ME}_{\text{AMEnew}}$ [keV]	influence [%]
^{76}Sr	-54 249(34)*	-54 390(298) #	-54 244(37)*	100
^{77}Sr	-57 804 (8)	-57 877(150)	-57 804 (8)	100
^{80}Sr	-70 322(14)	-70 304.4(7.5)	-70 308.2(6.6)	22
^{81}Sr	-71 532(11)	-71 526.1(7.5)	-71 527.7(6.2)	32
^{86}Sr	-84 520(12)	-84 521.6(2.2)	-84 521.6(2.2)	0
^{88}Sr	-87 920(10)	-87 919.7(2.2)	-87 919.7(2.2)	0
^{124}Sn	-88 228(20)	-88 236.1(1.4)	-88 236.1(1.4)	0
^{129g}Sn	-80 594(29)	-80 630(122)	-80 594(29)	95
^{130g}Sn	-80 136(10)	-80 232(27)	-80 141(11)	80
^{131g}Sn	-77 363(72)	-77 341(27)	-77 341(27)	0
^{132}Sn	-76 542(17)	-76 577(24)	-76 554(14)	67

Extrapolated with help of general trends

* The difference is due to rounding in an early stage of the evaluation

including only those contributions for which the spectra could be dedicated to the appropriate nuclear states of mother and daughter nuclide in an unambiguous way, a new average value for the β -decay of ^{130}Sb was obtained; $Q(\text{Sb} \rightarrow \text{Te}) = 5013(33)$ keV. The deviation of the spectroscopy data ($Q_{(\text{Sn} \rightarrow \text{Sb})} + Q_{(\text{Sb} \rightarrow \text{Te})}$) from the direct measured values ($m(\text{Sn}) - m(\text{Te})$) is now only 1.4σ .

In the case of ^{131}Sn , the increase of the uncertainty in accounting for the unresolved isomeric state makes the value as determined in this work ($\text{ME}(^{131g}\text{Sn}) = -77\,363(72)$ keV) to be of no weight for the adjustment. For ^{132}Sn two values for the mass excess were determined by Q_β -measurements [34]. From them, an AME-value $\text{ME}(^{132}\text{Sn}) = -76\,577(24)$ keV was derived. The data reported in this work shift the AME-value to be $\text{ME}_{\text{AMEnew}}(^{132}\text{Sn}) = -76\,542(17)$ keV, hence supporting the earlier Q_β -measurements.

5 Summary and Outlook

Using the Penning trap mass spectrometer ISOLTRAP at ISOLDE/CERN, the atomic masses of neutron-deficient strontium and neutron-rich tin isotopes

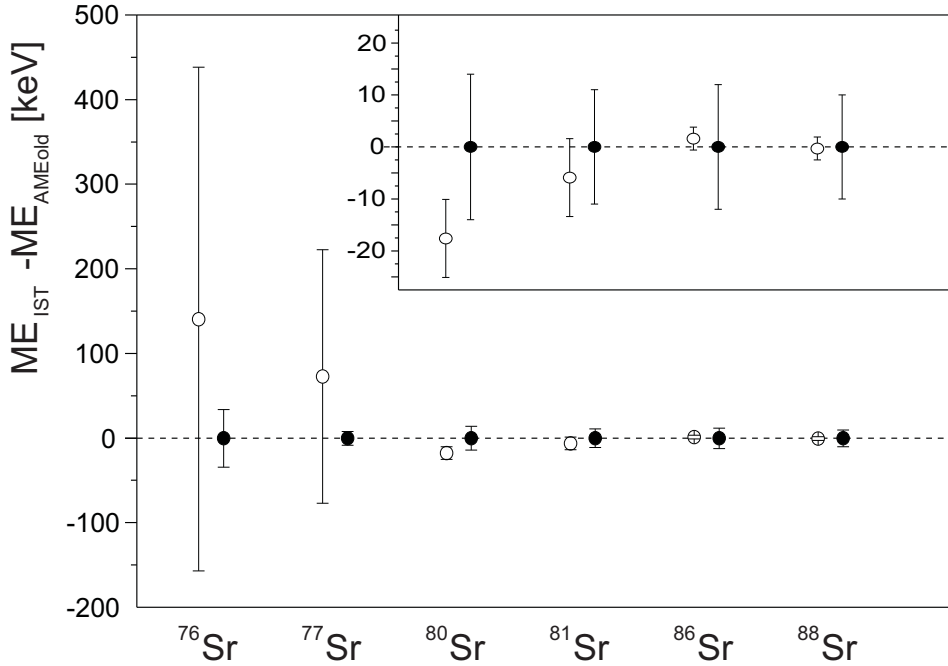


Fig. 5. Comparison of the new ISOLTRAP data ME_{IST} with the previous AME-values $\text{ME}_{\text{AMEold}}$ for the investigated Sr isotopes. The difference between the ISOLTRAP-value and the AME-value (not including ME_{IST}) is displayed as open circles for each isotope. The error bar represents the uncertainty of the AME values only. Next to each point the uncertainty of the ISOLTRAP measurement is given as the error bar of the filled circle. The inset shows on an enlarged scale the data for $^{80,81,86,88}\text{Sr}$.

were measured. The data were included into the new AME2003 mass adjustment [25] leading to an enhancement of the accuracy of the mass excess values in most of the studied cases. In Fig. 5 (for Sr) and Fig. 6 (for Sn) the difference of the values as given by the AME before the incorporation of the trap data and the ISOLTRAP values is displayed for each of the investigated nuclides.

The mass uncertainty of ^{77}Sr was decreased considerably and the mass excess of ^{76}Sr was measured for the first time. In the cases of $^{129,132}\text{Sn}$ the measurements reported here led to a decrease of the recommended mass value. For ^{130}Sn a significant deviation from the previously accepted value was found and resolved. The isomeric state of ^{131}Sn could not be resolved from the ground state. One possible reason for this is that the excitation energy is considerably smaller than the accepted value ($E_\gamma = 241.8(8)$ keV [28]). Theoretical shell model calculations support this assumption [35]. It is planned to repeat the mass measurement of ^{131}Sn at ISOLTRAP with higher resolving power to identify the two isomeric states of this nuclide.

The limitation during the Sn measurements due to isobaric contaminations, which made it impossible to access ^{133}Sn and heavier isotopes, can be tackled by using the high-resolution separator (HRS) at ISOLDE. It reaches a resolv-

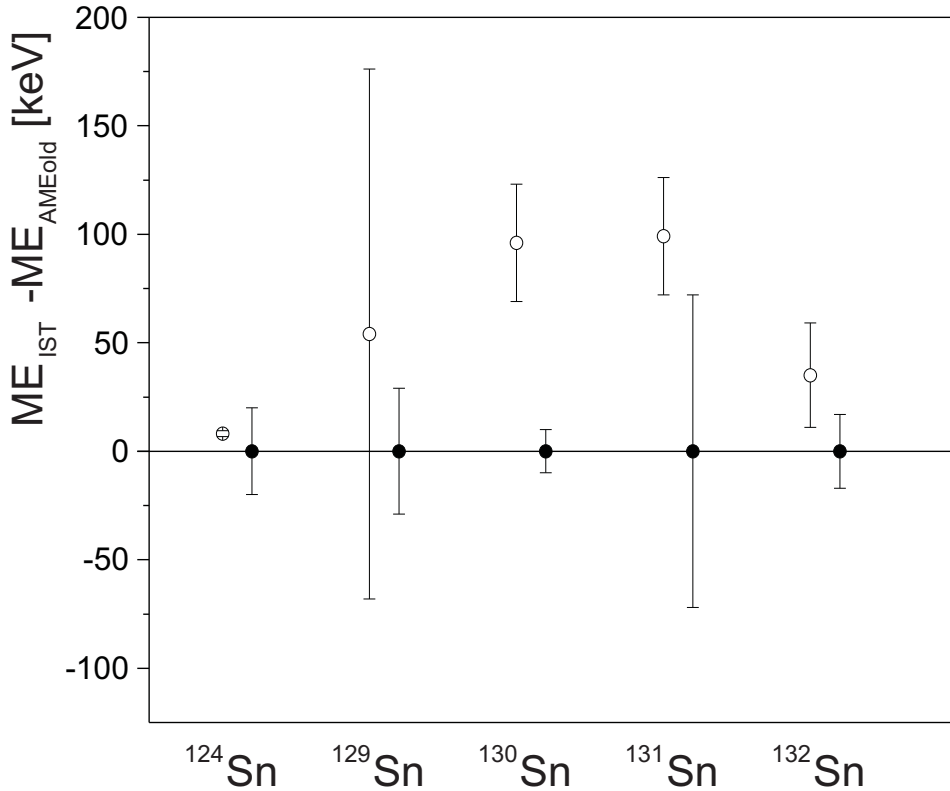


Fig. 6. Comparison of the new ISOLTRAP data ME_{IST} with the previous AME-values $\text{ME}_{\text{AMEold}}$ for the investigated Sn isotopes. For an explanation please see caption of Fig. 5.

ing power of $R \approx 7000$, which is considerably larger than the one of the general purpose separator (GPS) that was used for the measurements reported here.

The authors thank the ISOLDE technical group for assistance during the experiments. The support of the German Ministry of Education and Research (BMBF) as well as the support by the European Commission (EURO-TRAPS FMRX-CT-97-0144, RTD project EXOTRAPs FMGC-ET-98-0099, and HPRI program HPRI-CT-1998-00018) are gratefully acknowledged.

References

- [1] J. Dobaczewski et al., Phys. Rev. Lett. **72**, 981 (1994).
- [2] B. Chen et al., Phys. Lett. **B 355**, 37 (1995).
- [3] E. Wigner, Phys. Rev. **51**, 106 (1937).
- [4] F. Hund, Z. Phys. **105**, 202 (1937).
- [5] P. Van Isacker et al., Phys. Rev. Lett. **74**, 4607 (1995).
- [6] W. Satula et al., Phys. Lett. **B 407**, 103 (1997).
- [7] I. Hamamoto et al., Z. Phys. **A 353**, 145 (1995).
- [8] P. Sarriguren et al., Nucl. Phys. **A 691**, 631 (2001).
- [9] H. Schatz et al., Phys. Rep. **294**, 167 (1998).
- [10] J.M. D’Auria et al., Proc. of 14th Int. Conf. on Electromagnetic Isotope Separators and Techniques Related to their Applications, Victoria, BC, Canada, 6 - 10 May 2002, Nucl. Instr. Meth. **B 204**, 1 (2003).
- [11] D. Lunney et al., Rev. Mod. Phys. **75**, 1021 (2003).
- [12] G. Bollen et al., Nucl. Instr. Meth. **A 368**, 675 (1996).
- [13] E. Kugler, Hyp. Int. **129**, 23 (2000).
- [14] F. Herfurth et al., Nucl. Instr. Meth. **A 469**, 254 (2001).
- [15] H. Raimbault-Hartmann et al., Nucl. Instr. Meth. **B 126**, 378 (1997).
- [16] G. Savard et al., Phys. Lett. **A 158**, 247 (1991).
- [17] G. Gräff et al., Z. Phys. **297**, 35 (1980).
- [18] M. König et al., Int. J. Mass Spec. **142**, 95 (1995).
- [19] G. Audi and A.H. Wapstra, Nucl. Phys. **A 595**, 1 (1995).
- [20] G. Audi et al., Nucl. Phys. **A 624**, 1 (1997).

- [21] M.P. Bradley et al., Phys. Rev. Lett. **83**, 4510 (1999).
- [22] A. Kellerbauer et al., Eur. Phys. J. **D 22**, 53 (2003).
- [23] L.G. Smith and A.H. Wapstra, Phys. Rev. **C 11**, 1392 (1975).
- [24] CODATA, <http://physics.nist.gov/cuu/Constants/> (1998).
- [25] G. Audi et al., Nucl. Phys. **A 729**, 337 (2003).
- [26] T. Otto et al., Nucl. Phys. **A 567**, 281 (1994).
- [27] Y.V. Sergeenkov, Nucl. Data Sheets **58**, 765 (1989).
- [28] B. Fogelberg and J. Blomqvist, Phys. Lett. **B 137**, 20 (1984).
- [29] B.G. Kiselev et al., Sov. J. Nucl. Phys. **14**, 139 (1972).
- [30] L.L. Nunnelley and W.D. Loveland, Phys. Rev. **C 15**, 444 (1977).
- [31] E. Lund et al., Nucl. Phys. **A 286**, 403 (1977).
- [32] U. Stoeckler et al., Z. Phys. **A 336**, 369 (1990).
- [33] W.B. Walters and C.A. Stone, presented at the workshop on Nuclear Fission and Fission-Product Spectroscopy, Seyssins, France, 1994.
- [34] B. Fogelberg et al., Phys. Rev. Lett. **82**, 1823 (1999).
- [35] J. Genevey and J.A. Pinston, Laboratoire de Physique Subatomique et de Cosmologie, IN2P3-CNRS/Université Joseph Fourier, F-38026 Grenoble Cedex, France, private communication (1999).